Applied Physics A (2019) 125:757
https://doi.org/10.1007/s00339-019-3057-z

Applied Physics A
Materials Science & Processing

Thermoelectric properties of $CeNi_2Al_3$ compound: an experimental and theoretical study

A. Szajek[1] · **A. Kowalczyk**[1]

Received: 9 May 2019 / Accepted: 2 October 2019 / Published online: 12 October 2019

Abstract
We present thermoelectric properties of the $CeNi_2Al_3$ compound in the temperature range from 4 to 300 K. The electrical resistance (ρ) exhibits a metallic-like character reaching approximately 50 μΩ cm at room temperature. The temperature dependence of the Seebeck coefficient (S) is typical for mixed valence compounds having positive values with a broad maximum (~46 μV/K) over a wide temperature range from 200 to 300 K. The thermal conductivity (κ) value reaches 15 W/(m K) at $T = 300$ K. The power factor ($PF = S^2/\rho$) at 150 K is high (~70 μW/cm K^2), larger than for conventional thermoelectric materials based on Bi_2Te_3. The dimensionless figure of merit (ZT) has a broad maximum over a wide temperature range, which reaches the value of 0.1 around 220 K. The experimental results are supported by calculations within the density functional theory (DFT) performed on the basis of the full-potential local-orbital minimum-basis scheme (FPLO). The coherent potential approximation (CPA) is used to simulate the chemical disorder. The calculations are focused on the site preference of Ni and Al atoms. Investigations of the energetic stability have shown that in $CeNi_2Al_3$ the aluminum atoms prefer the 3g sites and the nickel ones the 2c sites.

1 Introduction

The efficiency of thermoelectric materials is estimated by the magnitude of the dimensionless parameter of the thermoelectric figure of merit $ZT = S^2T/\rho\kappa$, where S is the Seebeck coefficient (thermopower), σ is the electrical conductivity, and κ is the thermal conductivity. A good thermoelectric material should have high electrical conductivity, low thermal conductivity and a high Seebeck coefficient for maximum conversion of heat to electrical power or electrical power to cooling. The thermoelectric material most often used in today's Peltier coolers is an alloy of Bi_2Te_3 with $ZT \sim 1$. The power factor $PF = S^2/\rho$, is also an important parameter to optimize, related only to the electronic properties of the material.

At present, most thermoelectric (TE) materials are semiconductors, but it has been shown that some intermediate valence (IV) compounds, such as $YbAl_3$ [1, 2], also exhibit good thermoelectric properties at low temperatures. Intermediate valence alloys typically have metallic resistivities, but occasionally also show unusually large peaks in the Seebeck coefficient at low temperatures [3].

$CeNi_2Al_3$ is an intermediate valence compound with an unstable f-shell of the Ce ions [4]. It crystallizes in the hexagonal $PrNi_2Al_3$ type structure and exhibits metallic-like behavior [5]. As was generically observed in many IV compounds [6], $CeNi_2Al_3$ exhibits large thermopower (~40 μV/K) over a wide temperature range [7]. Upon Cu doping at Ni site, it shows simultaneous optimization of thermoelectric parameters [7, 8].

In this work, the thermoelectric properties of $CeNi_2Al_3$ system are studied to evaluate his potential for thermoelectric applications. Since thermopower is sensitive to behavior of conduction electrons in the vicinity of the Fermi level we will provide some data on the valence band based on an ab initio calculations. Also, the site preference by Ni and Al atoms is considered.

✉ A. Szajek
szajek@ifmpan.poznan.pl

A. Kowalczyk
ankow@ifmpan.poznan.pl

[1] Institute of Molecular Physics, Polish Academy of Sciences, ul. Mariana Smoluchowskiego 17, 60-179 Poznań, Poland

2 Experimental and computational details

High purity Ce (99.9%), Ni (99.9%) and Al (99.999%) elements were used to synthesize the $CeNi_2Al_3$ intermetallic compound by arc-melting in Ar atmosphere. The ingredients were remelted several times to ensure homogeneity. The weight of ingot was controlled to preserve nominal composition. The crystal structure was determined by a powder X-ray diffraction technique, using Cu-K_α radiation. The unit cell is hexagonal of the $PrNi_2Al_3$-type (symmetry *P6mmm,* Space Group no. 191). After X-ray diffraction and EDAX analysis it can be determined that the content of the impurity $CeAl_2$ phase is about 2%, as in previous studies [8] (Fig. 1).

All experimental results presented in this paper were made using a commercial multi-purpose measurement device (PPMS, manufactured by Quantum Design, San Diego), which allows controlled temperature and magnetic field sweep mode. Thermoelectric power and thermal conductivity measurements were performed simultaneously in the temperature range between 4 and 300 K in zero magnetic field. The measurements were carried out on a bar-shaped sample of the size $1\times1\times6$ mm^3 using a four-probe method. The gold coated copper contact leads were established to the sample using electrically and thermally conductive epoxy H20E offered by Quantum Design.

The electronic band structure calculations of the $CeNi_2Al_3$ sample were carried out using the full potential local-orbital minimum-basis scheme (FPLO) [9, 10]. The utilized FPLO5.00 version of the code is the latest public version allowing for the calculations within coherent potential approximation (CPA) [11]. The CPA was used to computationally model a chemical disorder as introduced to crystal structure of $PrNi_2Al_3$-type by random distribution of Al and Ni atoms between 2*c* and 3*g* sites. Three types of atomic distributions were considered: (i) $[NiNi]^{2c}$ and $[AlAlAl]^{3g}$, (ii) $[AlAl]^{2c}$ and $[AlNiNi]^{3g}$, (iii) $[NiAl]^{2c}$ and $[NiAlAl]^{3g}$. The form of CPA implementation in the FPLO5 prevents us from applying full-relativistic scheme and allows to use only a scalar-relativistic one. Only (i) distribution was calculated in both schemes as ordered case. The calculations were performed in the local density approximation (LDA) with the Perdew and Wang form of the exchange–correlation potential [12]. The calculations were performed for the reciprocal space mesh containing 484 irreducible *k*-points from 8000 ($20\times20\times20$) within the irreducible wedge of the Brillouin zone using the tetrahedron method for integrations [13]. The selfconsistent convergence criteria were equal to 10^{-8} Ha for the total energy and for a charge density 10^{-6}. The calculations were carried out for experimental lattice constants: $a=5.329$ Å and $c=4.052$ Å.

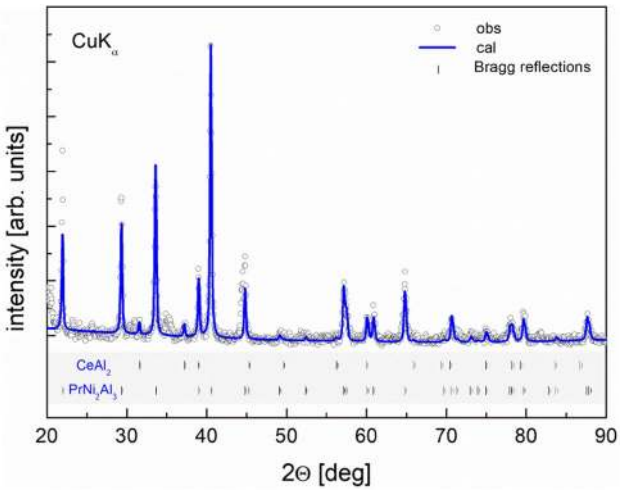

Fig. 1 Experimental (open dots) and calculated (blue solid line) X-ray powder diffraction patterns of the sample $CeNi_2Al_3$. The vertical bars correspond to the positions of the Bragg peaks of the main phases: $PrNi_2Al_3$-type and $CeAl_2$

3 Results and discussion

The general behaviour of $\rho(T)$ $CeNi_2Al_3$ shown in Fig. 2a shows the typical nature of metallic conductivity. The estimated value of the residual resistivity ratio (RRR) defined as the room temperature resistivity divided by $\rho(T\rightarrow0)$ is found to be 9, thus indicating the good quality of our sample. Room temperature value of $\rho(T)$ of our compound is 50 μΩ cm and is lower than the reported 350 μΩ cm for polycrystal $CeNi_2Al_3$ sample by Sun et al. [7]. Differences in electrical resistance and thermal conductivity are most likely due to the method in which the sample is obtained.

The character of the temperature dependence of the electrical resistivity is the same as in our work, but has much higher residual resistivity ρ_0 (~ 100 μΩ cm) [7]. Below 100 K, $\rho(T)$ follows the equation $\rho(T) = \rho_0 + aT^2$ with the parameters $\rho_0 = 5.6$ μΩ cm and $a=8.16*10^{-4}$ μΩ cm/K^2. The behaviour of the resistivity is characteristic of a Fermi liquid.

The temperature dependence of thermopower is shown in Fig. 2b and is typical of compounds with intermediate valence. Its extreme value of ~ 46 μV/K is obtained in a wide temperature range of 200–300 K, as in the case of Ref. [7, 8]. $S(T)$ is positive, indicating holes as dominant carriers in the temperature range 2–300 K, and its maximum value is similar to that reported previously for $CeNi_2Al_3$ [7, 8].

In Fig. 2b, one sees that the thermopower of $CeNi_2Al_3$ shows linear dependence $S=AT$ ($A=\pi^2k_B^2/3|e|$), up to about 25 K with $A=0.49$ μV/K^2, which is characteristic of thermopower in regime of Fermi liquid. This observation matches with the low temperature electrical resistivity which follows the Fermi liquid dependence of $\rho=aT^2$ (see Fig. 2a). The

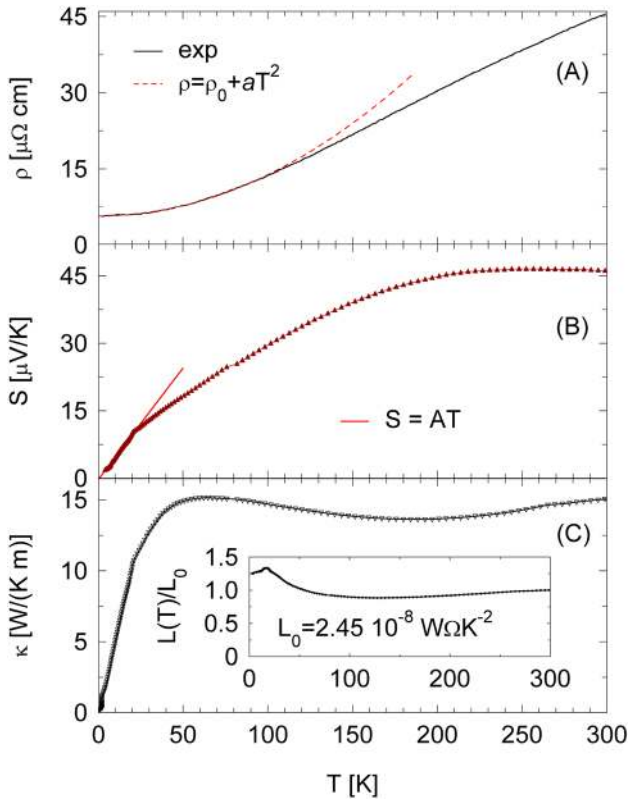

Fig. 2 The temperature dependence of the electrical resistivity (**a**), thermopower (**b**), and of the thermal conductivity (**c**). Inset: temperature dependence of the normalized Lorenz number L/L_0 scaled to unity at 300 K

deviation from the theoretical Mott model observed at higher temperatures ($T > 25$ K) may be connected with different scattering processes.

The temperature dependence of thermal conductivity $\kappa(T)$ of $CeNi_2Al_3$ is displayed in Fig. 2c. $CeNi_2Al_3$ is characterized by a broad maximum of $\kappa(T)$ at low temperatures, typical for metals and compounds. At low temperatures $\kappa(T)$ for $CeNi_2Al_3$ is linear relative to temperature, what is characteristic for electron scattering on lattice imperfections. Thermal conductivity value at the room temperature equal to 16 W/(m K) is larger compared to ~ 6 W/(m K) for $YbNiAl_4$ [14] and ~ 10 W/m K for $CeNi_2Al_3$ sample studied by Sun et al. [7]. Our κ values are comparable to hot-pressed polycrystalline $YbAl_3$ samples [2]. The thermal conductivity of $CeNi_2Al_3$ is large for two reasons: (a) there is a significant electronic contribution to κ because of the metallic nature of this compound, (b) its crystal structure is quite simple. One of the important ways to reduce thermal conductivity is to introduce disorder of mass distribution in the lattice to scatter phonons. As an example, it can be doped with Cu atoms, which increased TE properties at low temperatures [7]. In our case, further reduction of thermal conductivity, and in particular of the lattice component, as a result of the introduction of another type of atom as a disturbance will not significantly affect its value, because it is still negligible. The values of Lorenz number L have been calculated using the measured magnitudes of the total thermal conductivity κ and of the total electrical resistivity ρ and are represented in units of the Sommerfeld value $L_0 = 2.45 \times 10^{-8}$ W Ω K^{-2} of this quantity. Inset in Fig. 2c displays the reduced Lorenz number L/L_0 scaled to unity at room temperature to illustrate the Wiedemann–Franz law. The Lorenz number L shows only slight deviations from the theoretical value L_0 at low temperatures below 50 K. Such a tendency of L/L_0 was observed in RCu_4Au (R = Gd, Nd) [15] compounds and heavy fermion system $CeCu_4In$ [16]. The higher values of Lorentz number in alloys is due to phonon contribution to the thermal conductivity. At higher temperatures L/L_0 decreases and approaches the free-electron value of L_0. Since $L(T) \approx L_0$ for $CeNi_2Al_3$ the heat conductivity due to lattice vibrations seems to be of minor importance and can therefore be neglected at higher temperatures.

The quantities described above, such as electrical resistivity, thermopower, and thermal conductivity, are used to describe the transport properties of the tested material. However, for the description of thermoelectric properties, the following quantities are used: a power factor and a figure of merit defined as $PF = S^2/\rho$ and $ZT = S^2T/\rho\kappa$, respectively.

The power factor PF of $CeNi_2Al_3$ have a broad maximum (Fig. 3a) over a wide temperature range. The maximum value of $PF = 70$ μW/cm K^2 was obtained at 150 K. The PF value is greater than the values found for $YbNi_{4.2}Al_{0.8}$ of 45 μW/cm K^2 at 35 K [17], $Yb_2Pt_3Sn_5$ (43 μW/cm K^2 at 13 K) [18] and $NaCo_2O_4$ (50 μW/cm K^2) at room temperature [19]. The PF at 300 K is also quite high (41 μW/cm K^2) and comparable to that of conventional thermoelectric materials based on Bi_2Te_3 [19].

The quality of thermoelectric materials can be expressed by the dimensionless quantity figure of merit ZT. To get thermoelectric materials having large ZT values high power factors (S^2/ρ) and low thermal conductivity κ are required. However, it is found that some intermetallic compounds, such as $YbAl_3$, can also exhibit good thermoelectric performance. $CePd_3$ is perhaps the best example of a rare earth IV material, which has one of the largest ZT value at room temperature for this class of materials (~ 0.2 at 300 K) [20]. The values of ZT for $CeNi_2Al_3$ were calculated based on the temperature dependence of the Seebeck coefficient, electrical resistance and thermal conductivity (see Fig. 3b). Similar to the temperature dependence of thermopower, the ZT value for $CeNi_2Al_3$ exhibits a broad peak around 220 K reaching a maximum value of 0.1. The ZT value in our compound is higher in comparison to the that of reported by Sun et al. [7], because of the lower absolute value of electrical resistivity. It should be noted that the obtained thermoelectric values of ZT are reduced due to the high thermal conductivity.

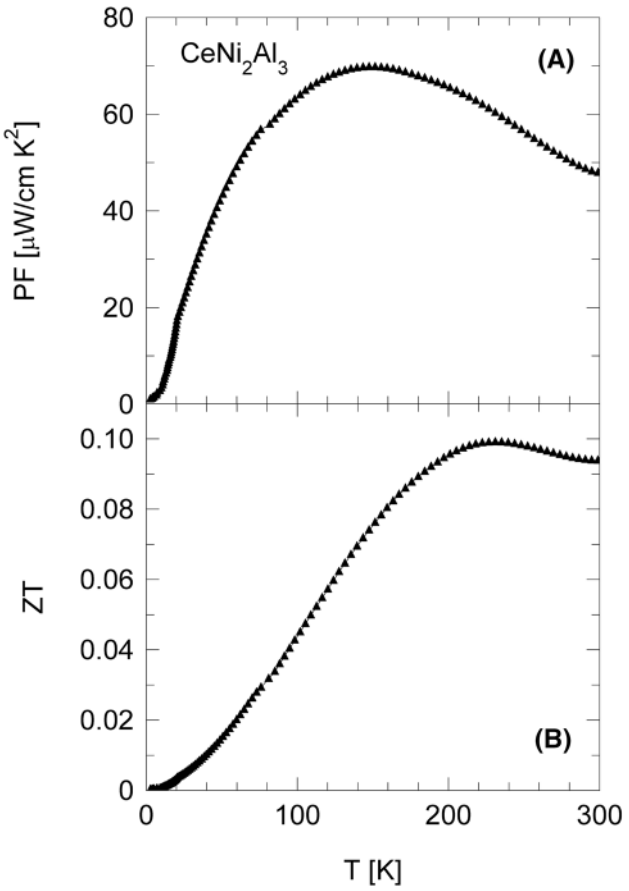

Fig. 3 The temperature dependences of power factor *PF* (**a**) and the dimensionless figure of merit *ZT* (**b**)

Sun et al. [7] reports that replacing Cu at the Ni site results in a simultaneous modification of the transport properties of $CeNi_{1.2}Cu_{0.8}Al_3$ so that the optimized parameter *ZT* obtains a value of 0.125 at 100 K. Finally, it is interesting to compare the values of *ZT* with similar group of compounds. Our maximum value of *ZT* of 0.1 at 220 K is comparable to that reported for CeRhSn at 180 K [21] and $YbAl_3$ [10], and is half of that reported for $CePd_3$ at 300 K [20], which is the highest value among IV compounds based on cerium atoms. Our *ZT* result for $CeNi_2Al_3$ is significantly better compared to other compounds: $FeSb_2$, $Fe_{0.95}Ir_{0.05}Si$, $CeAl_3$, and $CeCu_6$ [22–25].

Since thermopower is sensitive to behavior of conduction electrons in the vicinity of the Fermi level, some data on the valence band are necessary. The Mott two-band model for conduction and thermoelectric power usually gives reasonable estimates based on electronic structure data. However, in our case, the calculations from the first principles are limited to determining the preference of filling positions 2*c* and 3*g* by nickel and copper atoms. Site occupation as well as changes of lattice constants can give some insight into the possibilities of optimizing thermoelectric properties by changing the density of electronic states at the Fermi level. Such material engineering can be helpful in increasing the application value of the material being tested.

Ni and Al atoms occupy two sites in the unit cell: 2*c* and 3*g*. Regardless of distribution of Al and Ni atoms we assume Ce atoms always occupy 1a site. Then three possibilities take place: [i] system entirely ordered, $(NiNi)^{2c}$ and $(AlAlAl)^{3g}$; [ii] partially disordered in one position, $(AlAl)^{2c}$ and $(AlNiNi)^{3g}$; [iii] chemically disordered in both sites, $(NiAl)^{2c}$ and $(AlAlNi)^{3g}$. Performing calculations for these three cases one define the most stable distribution of Al and Ni atoms as well as important parameters for transport properties. They are collected in Table 1.

Received energies within ab initio calculations for three distributions of atoms marked as (i), (ii) and (iii) indicate that $CeNi_2Al_3$ goes to separation of different atoms in 2*c* and 3*g* sites. Disorder is not preferred. The energies for comparison were obtained within the same scheme: scalar relativistic calculations. Knowing that ordered distribution is preferred one can repeat calculations within fully relativistic scheme. Collected values in Table 1 and the DOS plots in Fig. 4 show that influence of relativistic corrections on $DOS(E=E_F)$ and shape of the valence band below the Fermi level is not significant. Characteristic for scalar relativistic calculations big single peaks above E_F formed by Ce(4*f*) electrons are visible. It is result of omission of spin–orbit coupling in this scheme. Including relativistic corrections the single peak is split into two peaks Ce($4f_{5/2}$) i Ce($4f_{7/2}$). Additionally peaks for disordered systems are broadened for results obtained in CPA.

The most interesting dependence of DOS is in vicinity of E_F because only electrons from this area can take part in transport. The last row of Table 1 contains the total $DOS(E_F)$ and the contributions provided by Ce, Ni and Al atoms. Despite the large number of Ni(3*d*) electrons, the nickel atoms do not provide the main contribution to the total value. During formation of $CeNi_2Al_3$ a charge transfer occurs from Ce and Al atoms. The Ni(3*d*) band fills up and moves towards higher binding energies and bottom of the valence band. Different situation is in the case of Ce atoms, the Ce(4*f*) band is almost empty and the greater part is located above E_F, this band crossing the Fermi level provides above 50% contribution to the total $DOS(E_F)$.

Knowledge of electronic structure gives opportunity to provide changes improving our material, for instance to increase $DOS(E_F)$. The first way is to introduce chemical disorder (see Table 1). The second one is granular structure of our material, changing size of grains one can manipulate the number of surface cells. These cells have slightly larger lattice constants. For this reason we performed calculations for systems having increased lattice constants (see table, cases $[i]^*$ and $[ii]^*$). Also in these cases $DOS(E_F)$ increases. The third way is to use rising curve of DOS above the Fermi level in Fig. 4. By replacing

Table 1 Electronic characteristics calculated for different atomic distributions [i], [ii] and [iii] (for details see explanations in the text) and experimental values of lattice constants $a = 5.329$ Å and $c = 4.052$ Å, otherwise ([i]* and [ii]*), the values are given below in table. ΔE: total energy related to the lowest energy -343442.7973878624 eV/f. u. obtained for case (i); DOS($E = E_F$): density of electronic states at the Fermi level; γ_0: calculated Sommerfeld coefficient

Distribution of Al and Ni atoms in 2*c* and 3*g* sites	$\Delta E = E - E_{(i)}$ [eV/f.u.]	DOS($E = E_F$) states/(eV f.u.)	γ_0 [mJ/(mol K^2)]
Scalar-relativistic calculations (within CPA)			
[i]	0.0000	5.050	11.91
[ii]	1.1643	7.440	17.54
[iii]	1.3282	6.627	15.63
[i] * a = 5.340 Å c = 4.052 Å	0.0272	5.088	11.99
[i] ** a = 5.340 Å c = 4.060 Å	0.0009	5.098	12.01
Fully relativistic calculations			
[i]	–	5.415 total (100%) 3.126 Ce (58%) 1.435 Ni (27%) 0.854 Al (15%)	12.76

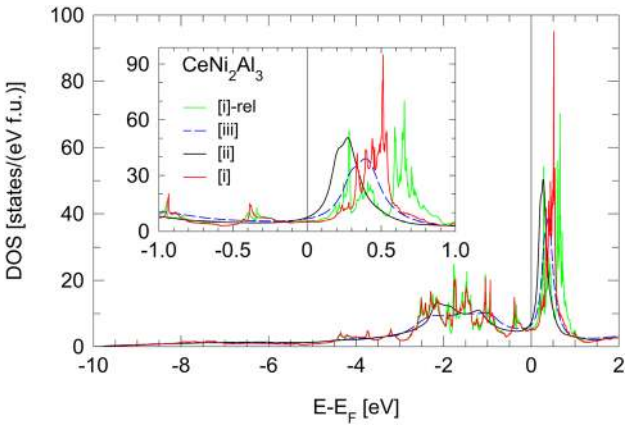

Fig. 4 DOS plots for the three types of atomic distributions: (i) $[NiNi]^{2c}$ and $[AlAlAl]^{3g}$, (ii) $[AlAl]^{2c}$ and $[AlNiNi]^{3g}$, (iii) $[NiAl]^{2c}$ and $[NiAlAl]^{3g}$. The calculations for [i] distribution were calculated for scalar-relativistic and fully relativistic modes. The inset presents results for energies close to the Fermi level

Cu atoms instead of Ni, one can insert additional electrons into the valence band, and then the Fermi level will shift to the right and DOS(E_F) will increase. Such situation has been confirmed experimentally [7, 26].

The position of the main peak formed by 4*f* electrons of cerium, Ce(4*f*), in relation to the Fermi level, obtained by ab initio calculations, is consistent with the results of fitting the TEP data in the temperature range 100–300 K to the two-band model proposed by Gottwick et al. [27]. The obtained values of E_F distance from Ce(4*f*) peak (Δ) and width of this band (Γ) do not differ from typical values for Ce and Yb compounds: $\Delta = 41$ meV and $\Gamma = 13$ meV.

4 Conclusions

Recently, the ternary compound $CeNi_2Al_3$ attracts much attention as a potential TE material. Not only has a metal-like resistivity of ~ 10^{-7} Ω m, but it also exhibits a fairly high absolute Seebeck coefficient of about 46 μV/K near room temperature. As a result, the $CeNi_2Al_3$ power factor reaches 70 μW/(cm K^2) at 150 K, which is higher than in the case of optimized Bi_2Te_3 based alloys. However, relatively large thermal conductivity (~ 16 W/(m K) at room temperature) lowers its figure of merit *ZT* (~ 0.1 at 220 K) due to its simple lattice.

The high power factor and the significant value of *ZT* is a strong impulse for further studies of $CeNi_2Al_3$ as a potential thermoelectric material. Knowledge of the electronic structure indicates that the application of new techniques to control material properties, techniques through nanostructuring and band engineering in the vicinity of the Fermi level, which usually lead to increase of *ZT* should be checked for their influence on the basic properties of the tested material. Therefore, further experimental and theoretical studies are necessary in this direction.

Acknowledgements The authors thank Dr. Z. Sniadecki for X-ray analysis of the sample and Mr. P. Skokowski for technical assistance.

References

1. K. Buschow, U. Goebel, E. Dormann, Phys. Status Solidi B Basic Res. **93**, 607 (1979)
2. D.M. Rowe, V.L. Kuznetsov, L.A. Kuznetsova, G. Min, J. Phys. D Appl. Phys. **35**, 2183 (2002)
3. V. Zlatić, R. Monnier, Phys. Rev. B **71**, 165109 (2005)
4. M. Coldea, M. Neumann, V. Pop, M. Demeter, J. Alloys Compd. **323–324**, 431 (2001)
5. R.J. Cava, A.P. Ramirez, H. Takagi, J.J. Krajewski, J. Magn. Magn. Mater. **128**, 124 (1993)
6. D. Jaccard, J. Sierro, in *Valence Instability*, ed. by P. Wachter, H. Boppart (Amsterdam, North-Holland, 1982), p. 409
7. P. Sun, T. Ikeno, T. Mizushima, Y. Isikawa, Phys. Rev. B **80**, 193105 (2009)
8. S. Yadam, D. Singh, D. Venkateshwarliu, M.K. Gangrade, S.S. Samatham, V. Ganesan, Phys. Status Solidi B **252**, 502 (2015)
9. K. Köpernik, H. Eschrig, Phys. Rev. B **59**, 1743 (1999)
10. K. Köpernik, B. Velický, R. Hayn, H. Eschrig, Phys. Rev. B **55**, 5717 (1997)
11. P. Soven, Phys. Rev. **156**, 809 (1967)
12. J.P. Perdew, Y. Wang, Phys. Rev. B **45**, 13244–13249 (1992)
13. P. Blöchl, O. Jepsen, O.K. Andersen, Phys. Rev. B **49**, 16223 (1994)
14. M. Falkowski, A. Kowalczyk, J. Appl. Phys. **123**, 175106 (2018)
15. A.K. Bashir, M.B.T. Tchokonte, A.M. Strydom, J. Magn. Magn. Mater. **414**, 69 (2016)
16. T. Tolinski, V. Zlatic, A. Kowalczyk, J. Alloys Compd. **490**, 15 (2010)
17. V.H. Tran, W. Miiller, A. Kowalczyk, T. Tolinski, G. Chełkowska, J. Phys. Condens. Matter **18**, 10353 (2006)
18. Y. Muro, K. Yamane, M.S. Kim, T. Takabatake, C. Godart, P. Rogl, J. Phys. Soc. Jpn. **72**, 1745 (2003)
19. I. Terasaki, Y. Sasago, K. Uchinokura, Phys. Rev. B **56**, R12685 (1997)
20. G. Mahan, B. Sales, J. Sharp, Phys. Today **50**, 42 (1997)
21. M.O. Kim, T. Sasakawa, Y. Echizen, T. Takabatake, Jpn. J. Appl. Phys. **42**, 6512 (2003)
22. A. Bentien, S. Johnsen, G.K.H. Madsen, B.B. Iversen, F. Steglich, Europhys. Lett. **80**, 17008 (2007)
23. B.C. Sales, E.C. Jones, B.C. Chakoumakos, J.A. Fernandez-Baca, H.E. Harmon, J.W. Sharp, E.H. Volckmann, Phys. Rev. B **50**, 8207 (1994)
24. M. Pokharel, T. Dahal, Z. Ren, P. Czajka, S. Wilson, Z.F. Ren, C. Opiel, Energy Convers. Manage. **87**, 584 (2014)
25. M. Pokharel, T. Dahal, Z.F. Ren, C. Opiel, J. Alloys Compd. **609**, 228 (2014)
26. S. Yadam, D. Singh, D. Venkateshwarlu, M.K. Gangrade, S.S. Samatham, V. Ganesan, Bull. Mater. Sci. **39**, 537 (2016)
27. U. Gottwick, K. Gloss, S. Horn, F. Steglich, N. Grewe, J. Magn. Magn. Mater. **47–48**, 536 (1985)